in: ***Boundary Elements XV,*** Proc. of the 15th Int. Conf. on Boundary Elements, Worcester, Massachusetts, USA, from 10 - 12 August 1993, pp.453−468

Nearly Singular and Hypersingular Integrals in the Boundary Element Method

Yijun Liu, Daming Zhang and Frank J. Rizzo
Center for Nondestructive Evaluation and
Department of Aerospace Engineering and Engineering Mechanics
Iowa State University, Ames, Iowa 50011, U.S.A.

ABSTRACT

Several techniques in dealing with nearly singular and hypersingular integrals which arise in applications of the boundary element method (BEM) are studied in this paper. The approach of using line integrals is emphasized and explored in some detail due to its high efficiency and accuracy. Numerical examples of stress analysis and scattering from an open crack in a 3-D elastic medium are presented to illustrate the ideas.

INTRODUCTION

Nearly singular integrals or nearly hypersingular integrals will occur in applications of the boundary element method whenever the source point is close to the surface (e.g., for 3-D problems) on which the integrations have to be performed. For example, nearly singular integrals will show up if one wants to evaluate interior displacement vectors at points close to the boundary of a body. Similarly, nearly hypersingular integrals, as well as nearly singular ones, will appear if one wants to evaluate interior stress tensors at these locations. On the other hand, nearly singular or hypersingular integrals can arise from boundary integral equation (BIE) formulations using either conventional BIEs or hypersingular BIEs, when parts of the boundary surface become close to one another, as in the cases of thin shapes or open cracks (cuts) in structures.

Accurate evaluation of nearly singular and hypersingular integrals is a demanding task since the integrands vary rapidly on the surface of integrations when the source point is close to this surface. The natural and most common practice in BEM applications is to use more integration (Gaussian) points (most often, lots of points) on the surface which is usually subdivided into small cells to ensure convergence. This simple approach certainly works but at a very high price. The computer time consumed by evaluations of these nearly singular or hypersingular integrals in this way is, in most cases, many times longer than that used by evaluations of other integrals. BEM programs,

otherwise efficient, become inefficient and unattractive when this approach is adopted for nearly singular or hypersingular integrals. Thus, for the boundary element method to stay competitive with other numerical methods, even for problems with thin shapes and cuts which have been regarded as unsuitable for BEM for a long time, new efficient procedures have to be developed to handle the nearly singular and hypersingular integrals arising in the BEM.

It is relevant to first mention the case of computations of singular and hypersingular integrals in the boundary element method. How to compute singular integrals in the BEM has been one of the focal points of research ever since the method was originated. Numerous research papers dealing with analytical and numerical treatments of the singular integrals were published in the literature during the last three decades. Analytical and numerical evaluations of the singular integrals (CPV) are either difficult to perform or require considerable care or computational effort. Hypersingular BIEs have been found very useful for many problems using the BEM (see, e.g. [1-9]). However, the direct evaluation of the hypersingular integrals, analytically or numerically, is even more troublesome. An alternative to direct evaluations is to recast the boundary integral equations, either singular or hypersingular, in terms of weakly singular integrals and then use regular integration quadrature to compute them. This has been the strategy in many of the works on elastostatics, elastodynamics and acoustics [10-17] using conventional and hypersingular BIEs. This strategy has been proven a successful one in dealing with singular and hypersingular integrals and is equally applicable to many other applications of the BEM.

The same thinking can be generalized to deal with *nearly* singular and *nearly* hypersingular integrals in the BEM. That is, one can transform these nearly singular integrals into nonsingular integrals or at most weakly singular integrals before applying any numerical quadrature. Three techniques are discussed in the following section for computing nearly singular and hypersingular integrals, namely, the kernel cancellation method, auxiliary surface method and the line integral method, all in the same spirit, that is, they exploit the properties of the kernel functions and avoid attacking the nearly singular or hypersingular integrals directly.

TECHNIQUES FOR NEARLY SINGULAR AND HYPERSINGULAR INTEGRALS

Kernel cancellation method

The idea of this method was originally brought to the attention of the authors by N. Nakagawa and further illustration and application of this idea in establishing weakly singular boundary integral equation formulations can be found in [18]. This idea is very simple and easy to implement for interior field evaluations. Let us consider the potential (or heat conduction) problem in 3-D and suppose we want to evaluate the potential ϕ (or temperature) at an interior point P_o (x_{ok}) close to the boundary S. The most commonly used integral representation is

$$\phi(P_o) = \int_S G(P,P_o)\frac{\partial\phi(P)}{\partial n}dS(P) - \int_S \frac{\partial G(P,P_o)}{\partial n}\phi(P)dS(P) \qquad (1)$$

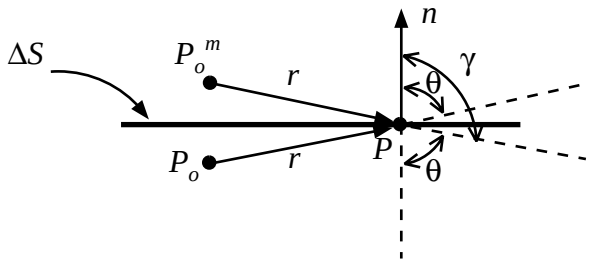

Fig. 1 The source point P_o and its mirror image P_o^m.

where $G(P,P_o) = 1/4\pi r$ ($r = |P_oP|$) and P (x_k) is the field point. Next, consider the following integral representation at the point P_o^m which is outside the body and is the 'mirror image' point of P_o about the surface S, Fig.1,

$$0 = \int_S G(P,P_o^m)\frac{\partial\phi(P)}{\partial n}dS(P) - \int_S \frac{\partial G(P,P_o^m)}{\partial n}\phi(P)dS(P). \qquad (2)$$

If we simply *add* the above two expressions, we obtain a new integral representation for the interior field $\phi(P_o)$,

$$\phi(P_o) = \int_S \left[G(P,P_o) + G(P,P_o^m)\right]\frac{\partial\phi(P)}{\partial n}dS(P) - \int_S \left[\frac{\partial G(P,P_o)}{\partial n} + \frac{\partial G(P,P_o^m)}{\partial n}\right]\phi(P)dS(P). \qquad (3)$$

The first integral in this representation is still nearly weakly singular when P_o is close to the surface. However, the second integral, which is originally nearly singular when P_o is close to the surface, is now a less singular integral since when P is on the small portion ΔS of the surface to which P_o is close,

$$\frac{\partial G(P,P_o)}{\partial n} + \frac{\partial G(P,P_o^m)}{\partial n} = -\frac{1}{4\pi r^2}\left(cos\theta + cos\gamma\right) = 0$$

assuming ΔS is locally flat (which is the case if S is smooth), Fig.1. By using the new integral representation (3), we can expect to get closer to the boundary than using the original representation (1), even though the nearly-weakly-singular-difficulty associated with the first integral still exists. This difficulty can be removed if a local polar coordinate transformation is introduced as for the weakly singular integrals [10].

By the same argument, we can expect to get closer to the boundary in the interior displacement field evaluation for elasticity problems, if the following alternative integral representation is employed,

$$u_i(P_o) = \int_S \left[U_{ij}(P,P_o) + U_{ij}(P,P_o^m)\right]t_j(P)dS(P) - \int_S \left[T_{ij}(P,P_o) + T_{ij}(P,P_o^m)\right]u_j(P)dS(P) \qquad (4)$$

where u_j and t_j are the displacement and traction vectors, respectively, and U_{ij} and T_{ij} the kernel functions (Kelvin solution).

Numerical tests presented in the next section using the integral representations (3) and (4), show considerable improvement in accuracy for the interior field evaluations at points close to the boundary. However, the generalization of this kernel cancellation idea to the integral representation for the interior stress evaluation is more complicated because of the complexity of the higher order kernels. For example, it is found that the success of the scheme (either adding or subtracting the two integral representations) for interior stress evaluation is a case by case situation, depending on the components of the stress sought and the type of boundary conditions near P_o.

Auxiliary surface method

This method utilizes the properties of the singular and hypersingular kernels and transforms nearly singular or hypersingular integrals on the original surface to integrals on an auxiliary surface which is further away from the source point such that the integrations are less demanding than the original ones. Take the T_{ij} integral on a surface ΔS as an example. ΔS may be one element or several elements near the source point P_o. Now, put an auxiliary surface ΔS^a (a 'bump' or a 'box') over ΔS such that $\Delta S \cup \Delta S^a$ forms a 'closed' surface, Fig.2. By the integral identities [14], which are simply statements of the properties of the T_{ij} and the hypersingular (derivatives of T_{ij}) kernels, the integral of T_{ij} (also that of the hypersingular) kernel over the surface $\Delta S \cup \Delta S^a$ (with normal pointing away from the region enclosed by $\Delta S \cup \Delta S^a$) is equal to zero since the source point is outside the region. Thus, we have the relation

$$\int_{\Delta S} T_{ij}(P, P_o) dS(P) = \int_{\Delta S^a} T_{ij}(P, P_o) dS(P) \tag{5}$$

where the normal on ΔS^a is in the same direction as that on ΔS. A similar relation holds for the hypersingular kernel.

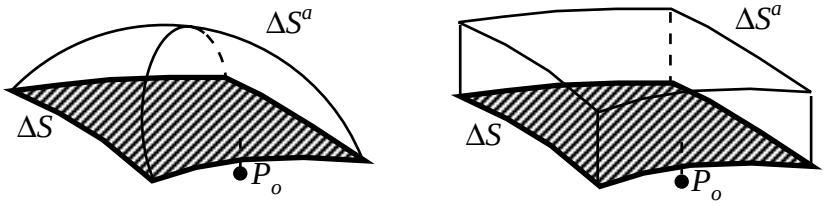

(a) A bump (b) A box

Fig. 2 Auxiliary surfaces over ΔS.

This auxiliary surface method works for both the nearly singular (or nearly hypersingular) integrals and the singular (or hypersingular) integrals (the limiting case as P_o tends to the boundary). It only requires constructions of the auxiliary surfaces and no new formulations need to be employed. However, the intensive numerical experiments conducted during this work reveal that the efficiency of this method is not satisfactory since subdivisions

on the auxiliary surfaces are still necessary in order to ensure convergence to correct numbers. The CPU time used for computing the integrals on these auxiliary surfaces can be sometimes several times longer than that used by computing all other integrals (nonsingular and singular integrals) during the formation of coefficient matrices.

Line integral method

In our experience, this approach is the most versatile and efficient method to deal with the nearly singular and hypersingular integrals. The basic idea is that one can use a Taylor series expansion of the density function to transform the nearly singular or nearly hypersingular integrals to nearly weakly singular ones plus some nonsingular line integrals. This idea was originally employed for computing hypersingular integrals [13] and has also been used for nearly singular and hypersingular integrals for thin body problems in acoustics [17].

First consider the following weakly singular form of the conventional BIE for 3-D *exterior* elastostatic problems [10,14], Fig.3(a),

$$u_i(P_o) + \int_S T_{ij}(P,P_o)\Big[u_j(P) - u_j(P_o)\Big]dS(P) = \int_S U_{ij}(P,P_o)t_j(P)dS(P). \quad (6)$$

For *interior* problems, the free term $u_i(P_o)$ in Eq.(6) will drop out. The two integrals in Eq.(6) are in general weakly singular integrals. Ordinary quadrature, together with local polar coordinate transformation, are sufficient to compute these integrals. However, if the surface in consideration is such that two parts of the surface become close to each other, such as the case shown in Fig.3(b), nearly singular integrals will arise from Eq.(6). Under this condition, the conventional BIE, in the form of Eq.(6), is no longer weakly singular. Special attention must be given to these nearly singular integrals.

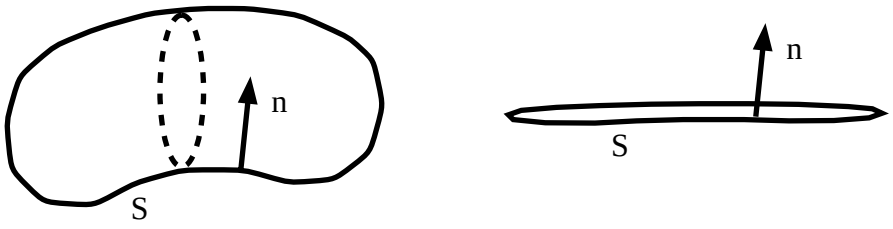

(a) A void in elastic medium (b) An open crack.

Fig. 3 Type of regions considered.

Now focus on a typical nearly singular integral in Eq.(6)

$$\int_{\Delta S} T_{ij}(P,P_o)u_j(P)dS(P)$$

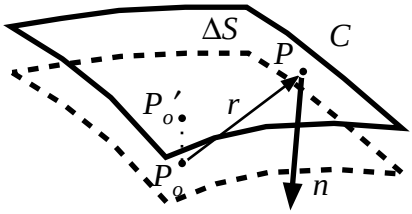

Fig. 4 An 'image point' P_o' on ΔS.

where ΔS is the part of the surface to which P_o is close. To transform this integral into a nearly weakly singular integral and line integrals, we first find an 'image point' P_o' on ΔS of the source point P_o, Fig.4, and then do the following subtraction of the density function about this image point,

$$\int_{\Delta S} T_{ij}(P,P_o)u_j(P)dS(P) = \int_{\Delta S} T_{ij}(P,P_o)\left[u_j(P) - u_j(P_o')\right]dS(P) + u_j(P_o')\int_{\Delta S} T_{ij}(P,P_o)dS(P)\,. \tag{7}$$

The first integral on the right hand side is a nearly weakly singular integral. We write the $T_{ij}(P, P_o)$ kernel in the form,

$$T_{ij}(P,P_o) = -\frac{1}{4\pi}\frac{1}{r^2}\frac{\partial r}{\partial n}\delta_{ij} + \frac{1}{4\pi}\left[\left(\frac{1}{r}\right)_{,j} n_i - \left(\frac{1}{r}\right)_{,i} n_j\right] + \frac{1}{8\pi(1-\nu)}\left[r_{,ikk}\,n_j - r_{,ikj}\,n_k\right]$$

where $(\ )_{,i} = \partial(\ )/\partial x_i$, and apply the Stokes theorem in the form

$$\int_{\Delta S} (\Psi_{,j}\,n_i - \Psi_{,i}\,n_j)\,dS = \epsilon_{ijk}\oint_C \Psi\,dx_k \tag{8}$$

where Ψ is a function defined on the surface ΔS, C the boundary (line) of ΔS (Fig.4) and $\in_{ijk}$ the permutation symbol. Then the last integral in (7) can be transformed into line integrals as follows

$$\int_{\Delta S} T_{ij}(P,P_o)dS(P) = I_\Omega(P_o)\,\delta_{ij} + \frac{1}{4\pi}\epsilon_{ijk}\oint_C \frac{1}{r}\,dx_k + \frac{1}{8\pi(1-\nu)}\epsilon_{jkl}\oint_C r_{,ik}\,dx_l \tag{9}$$

where

$$I_\Omega(P_o) = -\frac{1}{4\pi}\int_{\Delta S}\frac{1}{r^2}\frac{\partial r}{\partial n}\,dS \tag{10}$$

is a solid angle integral which can be readily converted to a line integral. Since

the source point P_o is always some distance away from the line C, all the line integrals are regular no matter how close P_o is to the surface ΔS. Thus, ordinary 1-D numerical integration scheme can be employed to compute these line integrals and fast convergence can be expected.

Next, consider the hypersingular BIE for 3-D *exterior* elastostatic problems (Fig.3(a)) written in the weakly singular form [16,14]

$$\begin{aligned} t_i(P_o) + \int_S H_{ij}(P,P_o)\left[u_j(P) - u_j(P_o) - \frac{\partial u_j}{\partial \xi_\alpha}(P_o)(\xi_\alpha - \xi_{o\alpha})\right] dS(P) \\ + E_{jklm}\, e_{\alpha l} \frac{\partial u_m}{\partial \xi_\alpha}(P_o) \int_S \left[K_{ij}(P,P_o) n_k + T_{ji}(P,P_o) n_{ok}\right] dS(P) \\ = \int_S \left[K_{ij}(P,P_o) + T_{ji}(P,P_o)\right] t_j(P) dS(P) - \int_S T_{ji}(P,P_o)\left[t_j(P) - t_j(P_o)\right] dS(P) \end{aligned} \tag{11}$$

in which ξ_α and $\xi_{o\alpha}$ (summation over α implied in (11), $\alpha = 1,2$) are the first two coordinates of P and P_o, respectively, in a local curvilinear coordinate system $O\xi_1\xi_2\xi_3$ which is defined on an element with ξ_1, ξ_2 in the tangential directions and ξ_3 in the normal direction, $e_{\alpha l} = \partial \xi_\alpha / \partial x_l$ is evaluated at P_o and

$$H_{ij}(P,P_o) = E_{iklm} \frac{\partial T_{lj}(P,P_o)}{\partial x_{om}} n_{ok}, \qquad K_{ij}(P,P_o) = E_{iklm} \frac{\partial U_{lj}(P,P_o)}{\partial x_{om}} n_{ok},$$

where E_{iklm} is the elastic constant tensor and n_{ok} the normal components at the source point P_o. The kernel H_{ij} is hypersingular (of the order $O(1/r^3)$) and the kernel K_{ij}, similar to T_{ij}, is strongly singular (of the order $O(1/r^2)$) (Expressions for H_{ij} and K_{ij} can be found in [16]). However, Eq.(11) is written in such a way that all integrals are at most weakly singular and no special integration schemes are needed to compute them, as long as the volume enclosed by the surface S is 'bulky', as shown in Fig.3(a). If the volume becomes 'thin', as shown in Fig.3(b), some of the integrals in Eq.(11) will no longer be weakly singular when the source point P_o is near but not on the surface of integration, Fig.4. Nearly hypersingular integrals of the following type

$$\int_{\Delta S} H_{ij}(P,P_o) u_j(P) dS(P)$$

will arise from Eq.(11) and need to be dealt with carefully. Similarly to what we have done to the nearly strongly singular integral, we first use the two term Taylor series expansion of the displacement vector about an image point P_o' (Fig.4), as follows,

$$\begin{aligned} \int_{\Delta S} H_{ij}(P,P_o) u_j(P) dS(P) \\ = \int_{\Delta S} H_{ij}(P,P_o)\left[u_j(P) - u_j(P_o') - \frac{\partial u_j}{\partial \xi_\alpha}(P_o')(\xi_\alpha - \xi_{o\alpha}')\right] dS(P) \\ + u_j(P_o') \int_{\Delta S} H_{ij}(P,P_o) dS(P) + \frac{\partial u_j}{\partial \xi_\alpha}(P_o') \int_{\Delta S} H_{ij}(P,P_o)(\xi_\alpha - \xi_{o\alpha}') dS(P). \end{aligned} \tag{12}$$

The first integral on the right hand side is a nearly weakly singular one when P_o is close to ΔS. We now transform the last two integrals into line integrals and nearly weakly singular integrals, and we write

$$\int_{\Delta S} H_{ij}(P,P_o)dS(P) = E_{iklm}\, n_{ok} \int_{\Delta S} \frac{\partial T_{lj}(P,P_o)}{\partial x_{om}} dS(P)$$

$$= -E_{iklm}\, E_{jnpq}\, n_{ok} \int_{\Delta S} \frac{\partial^2 U_{lp}}{\partial x_m \partial x_q}\, n_n dS$$

$$= -E_{iklm}\, E_{jnpq}\, n_{ok} \left\{ \int_{\Delta S} \left[\left(\frac{\partial U_{lp}}{\partial x_q} \right)_{,m} n_n - \left(\frac{\partial U_{lp}}{\partial x_q} \right)_{,n} n_m \right] dS \right.$$

$$\left. + \int_{\Delta S} \left(\frac{\partial U_{lp}}{\partial x_q} \right)_{,n} n_m\, dS \right\}.$$

Using the Stokes theorem (8) and noticing that

$$\Sigma_{ljn,\,n}(P,P_o) = 0$$

when $P_o \notin \Delta S$, where

$$\Sigma_{ljn}(P,P_o) = E_{jnpq} \frac{\partial U_{lp}(P,P_o)}{\partial x_q}$$

is the stress tensor in the Kelvin solution, we obtain

$$\int_{\Delta S} H_{ij}(P,P_o)dS(P) = E_{iklm}\, n_{ok}\, \epsilon_{mnr} \oint_C \Sigma_{ljn}(P,P_o)dx_r\,. \tag{13}$$

The transformation of the last integral in (12) is little more involved and the result is as follows

$$\int_{\Delta S} H_{ij}(P,P_o)(\xi_\alpha - \xi'_{o\alpha})dS(P)$$

$$= e'_{\alpha q}\, E_{iklm}\, n_{ok}\, \epsilon_{mnr} \oint_C \Sigma_{ljn}(P,P_o)(x_q - x'_{oq})dx_r$$

$$- e'_{\alpha n}\, E_{iklm}\, E_{jnpq}\, n_{ok}\, \epsilon_{mqr} \oint_C U_{lp}(P,P_o)dx_r$$

$$+ e'_{\alpha m}\, E_{iklm}\, n_{ok} \int_{\Delta S} T_{lj}(P,P_o)dS$$

$$- e'_{\alpha m}\, E_{jmlk}\, n_{ok} \int_{\Delta S} T_{li}(P,P_o)dS$$

$$+ e'_{\alpha l}\, E_{jlkm} \int_{\Delta S} \left[K_{im}(P,P_o)n_k + T_{mi}(P,P_o)n_{ok} \right] dS \tag{14}$$

where $e'_{\alpha l}$ is the same $e_{\alpha l}$ vector as in Eq.(11) but evaluated at the image point P_o'. The two line integrals in the above formula are regular and can be computed easily. The third and fourth integrals can be computed using line integrals as given in (9). The last integral in the above formula is a surface integral, very similar to the second integral in Eq.(11), and is nearly weakly singular no matter how close the source point P_o is to the surface ΔS.

To use the line integrals as presented in (9), (13) and (14) for the nearly singular and hypersingular integrals (also valid for the singular and hypersingular cases), much work is needed in computer programming. However, the resulting program is very efficient in computing these nearly singular or hypersingular integrals. It was found in a test that the CPU time used to compute the two integrals as given by (13) and (14) using the line integrals on one element was less than 2 seconds (on a DECstation 5000/240), while to compute the original surface integrals using many subdivisions took about 11 minutes in order to achieve the same accuracy (the distance of the source point to a square element is 0.01 and the element length is 2).

NUMERICAL EXAMPLES

Example 1. Potential evaluation using the kernel cancellation method

This example is designed to test the new integral representation for interior potential (or temperature) evaluation given by formula (3) using the kernel cancellation concept. The region (in 2-D) considered is shown in Fig.5. Only four quadratic line elements (one on each side) are used. The boundary conditions are: ϕ=300 along x=0, ϕ=0 along x=1, $\partial\phi/\partial n$=0 along both y=0 and y=1. The potential (or temperature) at selected interior points along y=0.5 and x=0.5 are plotted in Fig.6 and Fig.7, respectively, using both the original representation (1) and the new representation (3). Considerable improvement is achieved by using the new representation (3) at all places near the boundary where $\phi\neq 0$, but at x=1 (in Fig.6) where ϕ=0, the original small error is actually doubled due to the nearly *weakly* singular kernel doubled in (3) as compared with (1). Thus the new representation (3) is very helpful in getting close to the boundary where $\phi\neq 0$, but it is *not* helpful near the boundary where ϕ=0.

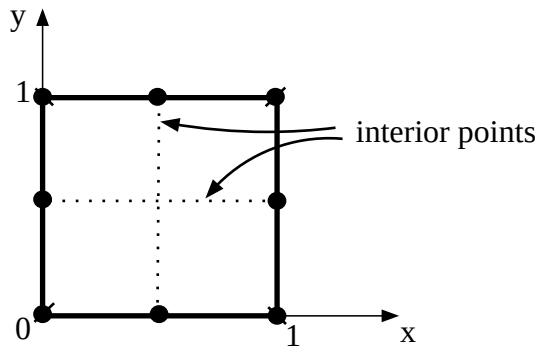

Fig. 5 A square region and four quadratic line elements.

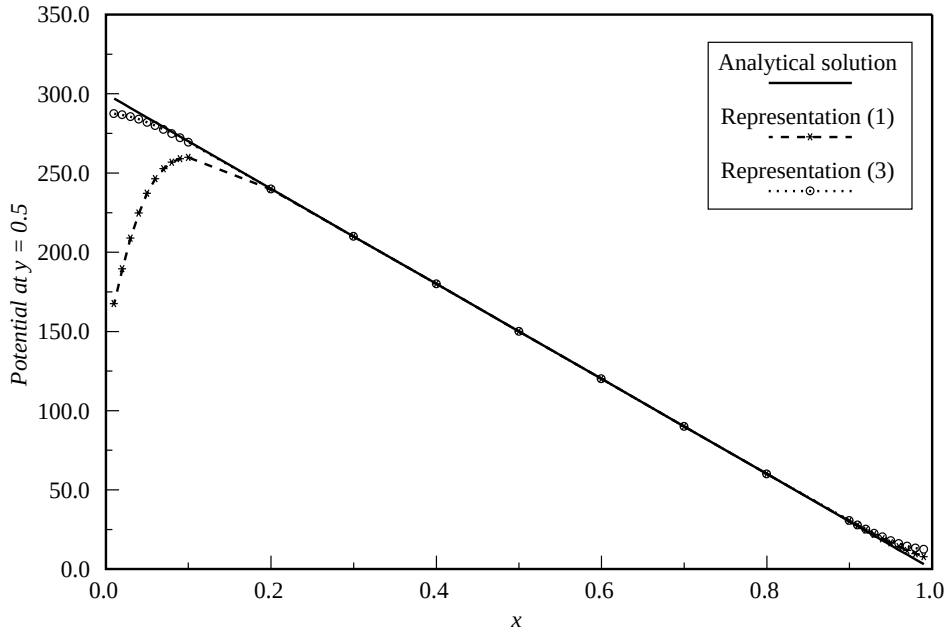

Fig. 6 Potential at points along the line y=0.5.

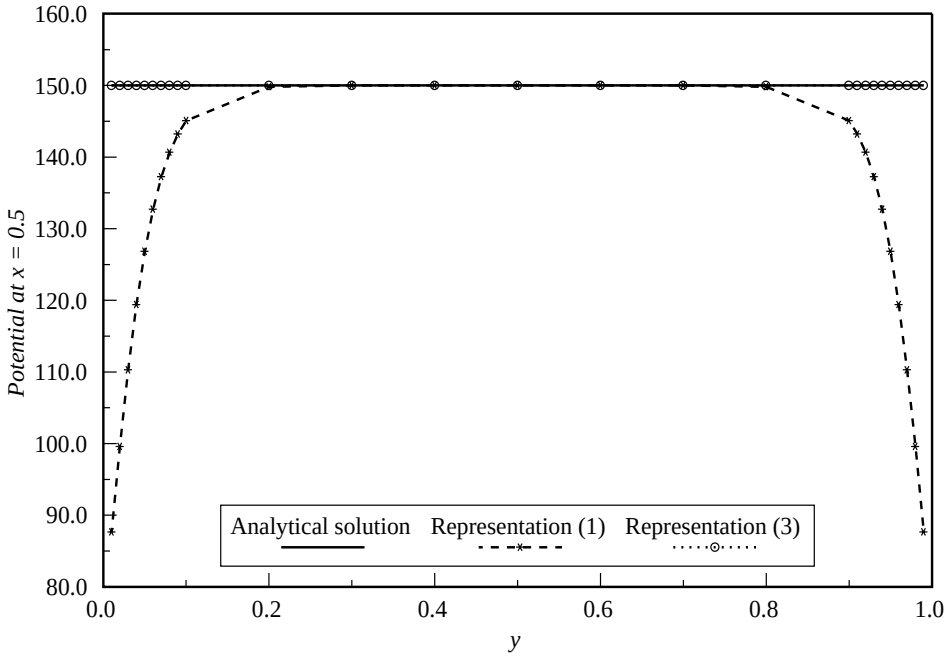

Fig. 7 Potential at points along the line x=0.5.

Example 2. Displacement evaluation using the kernel cancellation method

The same region and mesh as shown in Fig.5 is considered for a 2-D elasticity problem. The boundary conditions are: x-component of the displacement u=0 along x=0, y-component of the displacement v=0 at the point x=0 and y=0, u=1 along x=1 and zero tractions at all other directions and places. The displacement component u at points along the lines y=0.5 and x=0.5 are plotted in Fig.8 and Fig.9, respectively. As for the potential problem, we see substantial improvement at the points close to the boundary, except near x=0 in Fig.8, where the small error is doubled for new representation (4) due to the nearly weakly singular integrals. Similar results are observed for the displacement component v.

While the above results are preliminary, they are very encouraging. However, the outcome of the tests on the stress evaluation is mixed. Both the addition and subtraction of the interior and exterior integral representations were tested. At some locations some components of the stress exhibit significant improvement, while some components get worse at other locations. This complication is due to the complexity of the higher order kernel functions in the stress integral representation. Further investigation into this is under way.

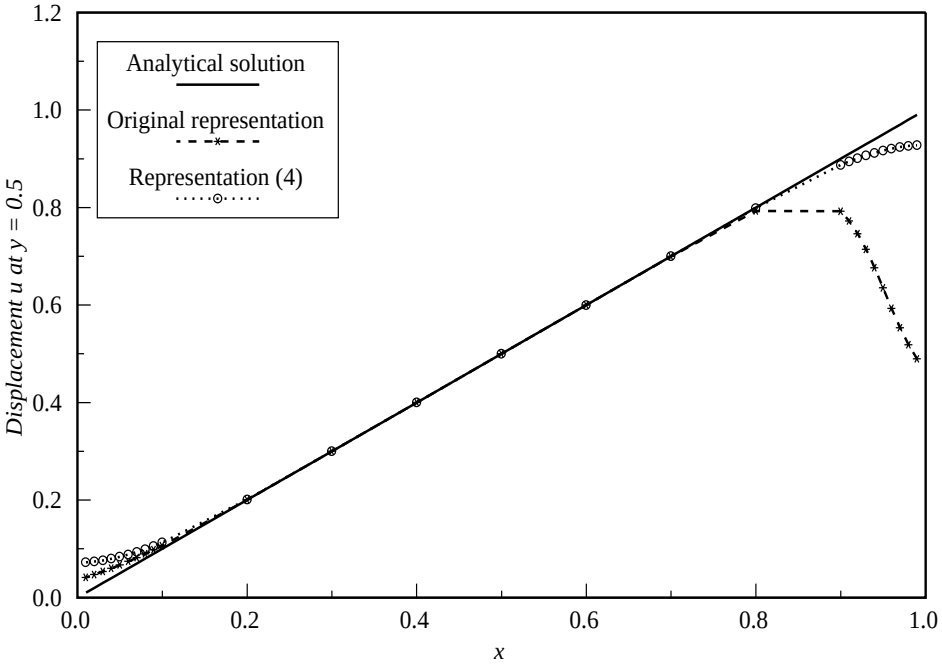

Fig. 8 Displacement component u at points along the line y=0.5.

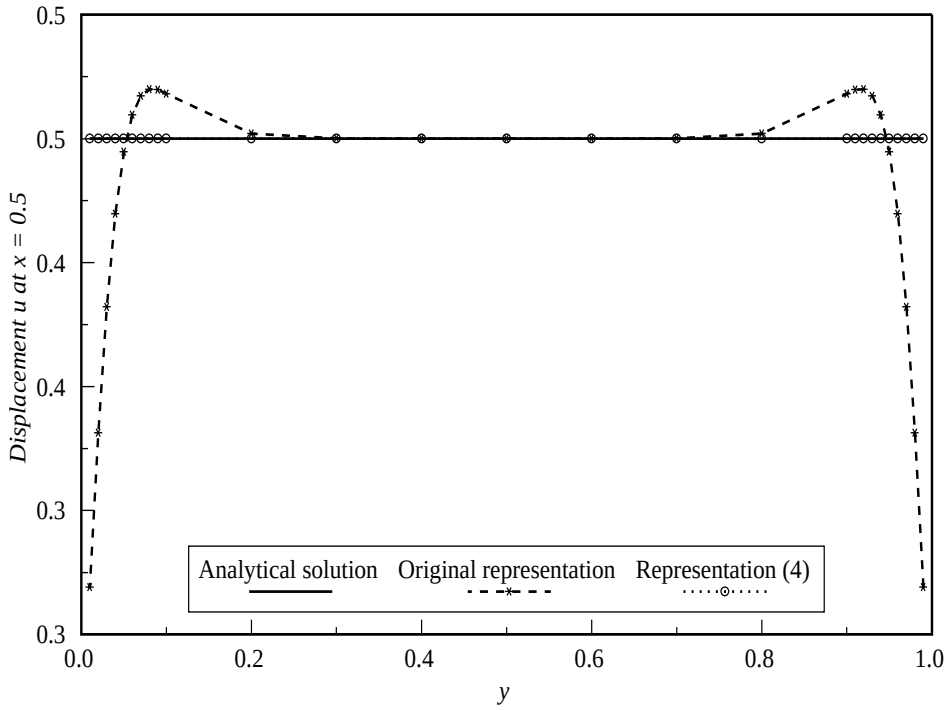

Fig. 9 Displacement component u at points along the line x=0.5.

Example 3. Cantilever beam with a cut

This example is intended to test the effectiveness of the use of line integrals for the nearly singular integrals in the conventional BIE. A cantilever beam with a cut (or an open surface crack) at the middle is loaded at the end with a uniform traction $t_2=q$, Fig.10. The dimension of the beam is B=1, H=1 and L=6. The cut has a depth of 1/2 and a varying opening ranging from 0.29 down to 0.0001. Conventional BIE (6) (without the free term) is used with (conforming) quadratic elements. It is emphasized that only four elements are used for the two surfaces of the cut and the mesh is only suitable for analysis of quantities away from the crack (e.g., the deflection at the end). Nearly singular integrals appear when the collocation point is on one surface of the cut and the integration of the singular kernel is on the other surface.

The deflection at the end of the beam is plotted in Fig.11 against the opening of the cut. One curve is the result using the line integrals in (9) for the nearly singular integrals and the other curve shows the result without doing anything special for the nearly singular integrals (just use the surface integration scheme as for nonsingular integrals). The two curves are in agreement when the cut is wide open, which suggests that the surface integrations are still acceptable at this stage. As the opening becomes smaller, the result employing line integrals stays about constant until the opening is reduced to about 0.1. On the other hand, the result using surface integrals

becomes decreasing, which is unreasonable since the opening of the cut should have little effect on the deflection at the end if the depth of the cut is fixed. This suggests that the surface integration scheme can not handle the nearly singular integrals when the two surfaces of the cut become close while the line integral approach works well. For references, the end deflection is 864*q/E* (*E* is Young's modulus) for the same cantilever beam without the cut, and is 1404*q/E* for a beam with a height of 1/2H from middle to the free end and a height of H from the middle to the fixed end (same B and L), according to the simple beam theory.

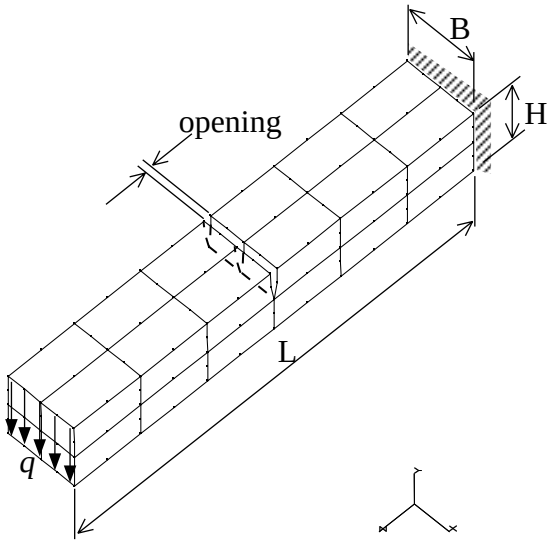

Fig. 10 BEM mesh for the cantilever beam with a cut.

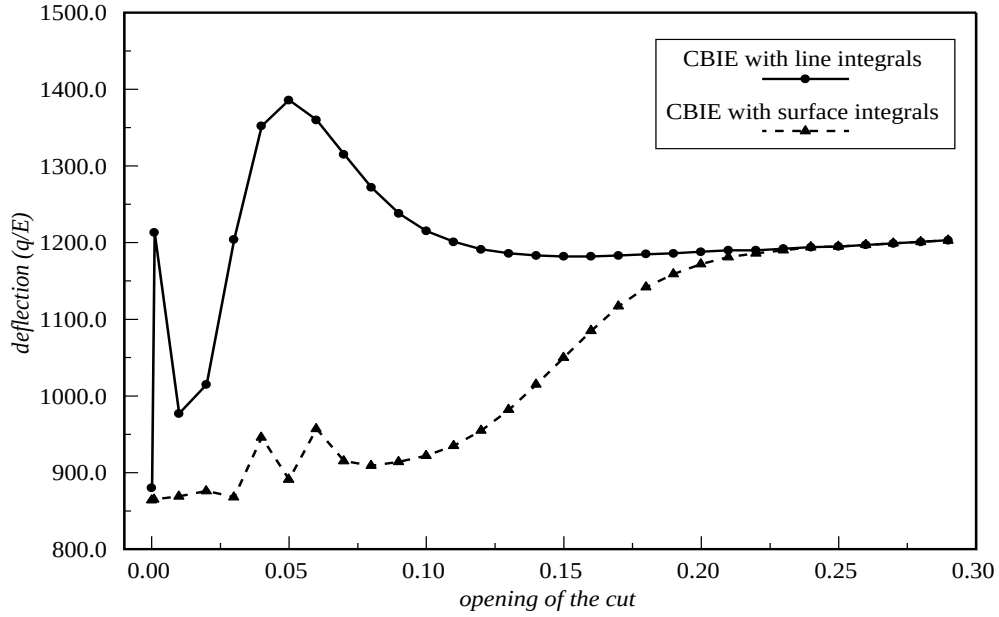

Fig. 11 Deflection of the end vs. different opening of the cut (ν=0.3).

When the opening is below about 0.1, the data using the line integrals becomes unstable too, because of the degeneracy of the conventional BIE for crack-like problems (see, e.g. [17]). This degeneracy is indicated by a sharp rise in condition numbers of the coefficient matrix when the opening is small. A nondegenerate system of equations for such problems can be obtained by incorporating hypersingular BIEs [17], as demonstrated in the next example.

Example 4. Scattering from a penny-shaped open crack in 3-D.

A penny-shaped open crack in a 3-D elastic medium is impinged upon by a plane longitudinal wave in the direction normal to the crack surfaces. The dynamic counterpart [11,16] of the conventional BIE (6) and the hypersingular BIE (11) are applied to form a composite BIE formulation which is nondegenerate for thin body problems [17]. Nearly singular and hypersingular integrals in these BIEs are computed by using the line integrals given in (9), (13) and (14). The CPU time used for computing these integrals is only a fraction of the time for all other singular and nonsingular integrals. The two surfaces of the open crack are discretized by a total of 32 nonconforming quadratic surface elements [13,15,16]. The scattering cross section at (shear) wave numbers $k_T a$=1,2,...,6 using the composite BIE formulation is plotted in Fig.12 for three different openings of the crack and compared with the analytical solution [19] (eight data points used). It is observed that the crack opening has little effect on the scattering cross section which is a far field quantity. The system of equations using the composite BIE is well-behaved in all the cases studied (low condition numbers are observed).

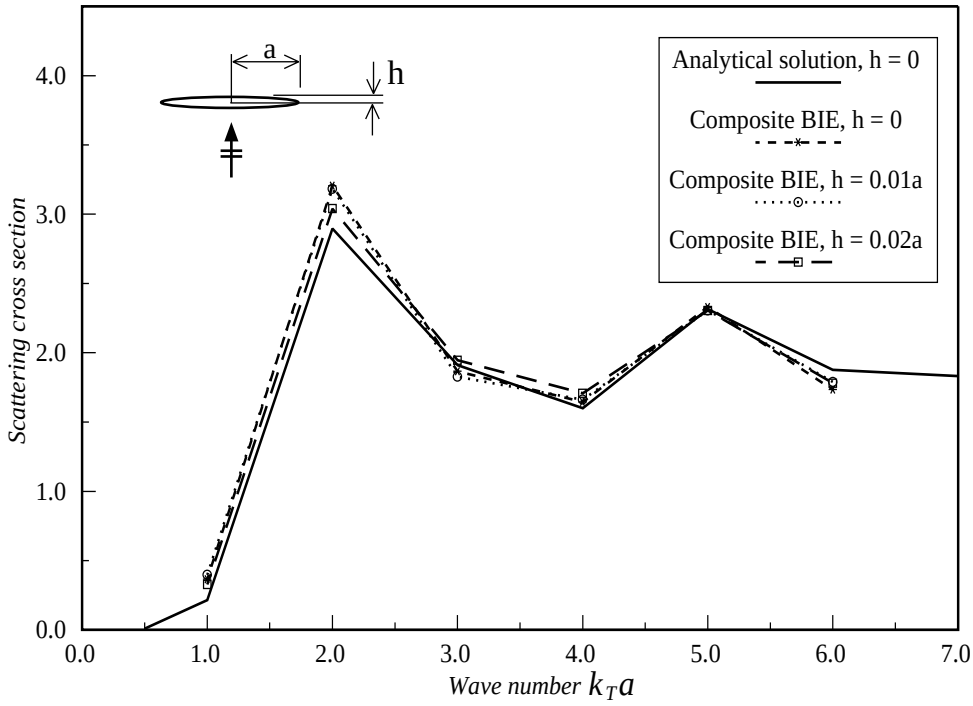

Fig. 12 Scattering cross section of a penny-shaped open crack.

CONCLUSIONS

Three methods for computing nearly singular or nearly hypersingular integrals in the BEM are studied in this paper. All three methods represent a departure from the commonly used numerical procedure in the BEM that directly computes the nearly singular or hypersingular integrals on original surfaces by employing subdivisions and a large number of integration points. The kernel cancellation method, which exploits the combinations of the interior and exterior integral representations, is easy to implement, efficient in computation and especially useful in the evaluation of interior fields. The auxiliary surface method, which transforms integrals on original surfaces to some auxiliary surfaces further away from the source point, is also relatively easy to implement but its efficiency is unsatisfactory. The line integral method, which transforms nearly singular or hypersingular integrals to sums of nearly weakly singular integrals and nonsingular line integrals, seems to be the most versatile and efficient approach to deal with the nearly singular or hypersingular integrals, as demonstrated by the numerical examples presented in this paper.

ACKNOWLEDGMENT

The authors would like to thank Drs. T. J. Rudolphi, G. Krishnasamy and N. Nakagawa for many discussions on hypersingular integrals and related topics. This work was sponsored by NIST under cooperative agreement #70NANB9H0916 and was performed at the Center for NDE, Iowa State University; and by the FAA-Center for Aviation Systems Reliability, operated by the Ames Laboratory, USDOE, for the Federal Aviation Administration under Contract No. W-7405-ENG-82 with Iowa State University.

REFERENCES

[1] A. J. Burton and G. F. Miller, 'The application of integral equation methods to the numerical solution of some exterior boundary-value problems,' *Proc. R. Soc. Lond.* A **323**, 201-210 (1971).

[2] K. Takakuda, T. Koizumi and T. Shibuya, 'On integral equation methods for crack problems,' *Bull. Jap. Soc. Mech. Engrs* **28**, 217-224 (1985).

[3] W. Lin and L. M. Keer, 'Scattering by a planar three-dimensional crack,' *J. Acoust. Soc. Am.* **82** (4), 1442-1448 (1987).

[4] N. I. Ioakimidis, 'Validity of the hypersingular integral equation of crack problems in three-dimensional elasticity along the crack boundaries,' *Engng Fract. Mech.* **26**, 783-788 (1987).

[5] N. Nishimura and S. Kobayashi, 'An improved boundary integral equation method for crack problems,' in: T. A. Cruse, ed., *Advanced Boundary Element Methods*, Springer-Verlag, New York (1988).

[6] P. A. Martin and F. J. Rizzo, 'On boundary integral equations for crack problems,' *Proc. R. Soc. Lond.* A **421**, 341-355 (1988).

[7] L. J. Gray, L. F. Martha and A. R. Ingraffea, 'Hypersingular integrals in boundary element fracture analysis,' *Int. J. Numer. Meth. Engng*, **29**, 1135-1158 (1990).

[8] C. C. Chien, H. Rajiyah and S. N. Atluri, 'An effective method for solving the hypersingular integral equations in 3-D acoustics,' *J. Acoust. Soc. Amer.*, **88**, 918-937 (1990).

[9] J. H. Kane and C. Balakrishna, 'Symmetric Galerkin boundary formulations employing curved elements,' to appear in *Int. J. Numer. Meth. Engng*.

[10] F. J. Rizzo and D. J. Shippy, 'An advanced boundary integral equation method for three-dimensional thermoelasticity,' *Int. J. Numer. Meth. Engng*, **11,** 1753-1768 (1977).

[11] F. J. Rizzo, D. J. Shippy and M. Rezayat, 'A boundary integral equation method for radiation and scattering of elastic waves in three dimensions,' *Int. J. Numer. Meth. Engng*, **21,** 115-129 (1985).

[12] T. J. Rudolphi, G. Krishnasamy, L. W. Schmerr and F. J. Rizzo, 'On the use of strongly singular integral equations for crack problems,' in: *Boundary Elements X*, C. A. Brebbia, ed., Comp. Mech. Pub., Southampton, 249-263 (1988).

[13] G. Krishnasamy, L. W. Schmerr, T. J. Rudolphi and F. J. Rizzo, 'Hypersingular boundary integral equations: some applications in acoustic and elastic wave scattering,' *J. Appl. Mech.*, **57**, 404-414 (1990).

[14] Yijun Liu and T. J. Rudolphi, 'Some identities for fundamental solutions and their applications to weakly-singular boundary element formulations,' *Engineering Analysis with Boundary Elements*, **8**, No.6 (1991).

[15] Yijun Liu and F. J. Rizzo, 'A weakly singular form of the hypersingular boundary integral equation applied to 3-D acoustic wave problems,' *Comp. Meth. in Appl. Mech. and Engng*, **96**, 271-287 (1992).

[16] Yijun Liu and F. J. Rizzo, 'Hypersingular boundary integral equations for radiation and scattering of elastic waves in three dimensions,' *Comp. Meth. in Appl. Mech. and Engng*, in press.

[17] G. Krishnasamy, F. J. Rizzo and Yijun Liu, 'Boundary integral equations for thin bodies,' *Int. J. Numer. Meth. Engng*., in press.

[18] N. Nakagawa, 'Near-surface field evaluation in two-phase Helmholtz problem,' to be presented at *IABEM-93 Symposium*, Braunschweig, Germany, August 16-19, 1993.

[19] P. A. Martin and G. R. Wickham, 'Diffraction of elastic waves by a penny-shaped crack: analytical and numerical results,' *Proc. R. Soc. Lond.* A **390**, 91-129 (1983).